[17] R. E. R. Colen, M. Kolodziejczyk, B. Delmon, J. H. Block, *Surf. Sci.* **1998**, *412*, 447 – 457.
[18] R. W. Vook, B. Oral, *Appl. Surf. Sci.* **1992**, *60*, 681 – 687.
[19] W. F. Egelhoff, Jr. in *The Chemical Physics of Solid Surfaces and Heterogeneous Catalysis*, *Vol. 4* (Eds.: D. A. King, D. P. Woodruff), Elsevier, Amsterdam, **1982,** pp. 397 – 426.
[20] K. C. Taylor, *Stud. Surf. Sci. Catal.* **1987**, *30*, 97 – 116.
[21] S. M. Vesecky, P. Chen, X. Xu, D. W. Goodman, *J. Vac. Sci. Technol. A* **1995**, *13*, 1539 – 1543.

The Hume – Rothery Compound $Mn_8Ga_{27.4}Zn_{13.6}$: Separated Zn_{13}-Clusters Interspersed in a Primitive Cubic Host Lattice**

Ulrich Häussermann,* Per Viklund, Christer Svensson, Sten Eriksson, Pedro Berastegui, and Sven Lidin

The interpretation of structural stability and chemical bonding in intermetallic compounds is a continuous challenge in chemistry because metallic systems evade the simple and powerful rules developed by chemists which allow the linking of electron counts to particular geometrical arrangements of atoms.[1, 2] However, there exists a number of intermetallic compounds where the valence electron concentration (VEC, average number of valence electrons per atom) plays a decisive role for structural stability, and these compounds are usually classified as electron compounds[3] or Hume – Rothery compounds.[4] One group of such Hume – Rothery compounds comprises E-rich systems T_mE_n ($n/m \geq 3$) where T is a transition metal from the V – Co groups and E is preferably Al or Ga. In these compounds the transition metal atoms appear uniformly distributed in a matrix of E atoms, and the resulting structures (e.g., VAl_{10}, WAl_{12}, $MnAl_6$, Co_2Al_9, $MnGa_4$, V_8Ga_{41}, V_7Al_{45}) are very often large and complex. Remarkably the T atoms are separated by the largest distance possible and, thus, are only coordinated by E atoms in the first coordination sphere. The resulting TE_p coordination polyhedra are rather regular ($p = 8 – 12$) and appear as discrete entities (VAl_{10}, WAl_{12}), as vertex-linked (Co_2Al_9, $MnGa_4$, V_8Ga_{41}), or as edge-linked ($MnAl_6$) networks. Many of these T_mE_n Hume – Rothery compounds were prepared and characterized 20 years ago, but have experienced a renaissance recently with the discovery of further examples such as $MoAl_6$, WAl_6, Mo_5Al_{22}, and the ternay $Mo_7Sn_{12}Zn_{40}$ by Hillebrecht et al.[5]

The origin of the important role of VEC for the stability of this group of Hume – Rothery compounds lies in the occurrence of a pronounced pseudo gap in the density of states (DOS) which is a result of strong bonding between T and E atoms.[6] We want to exemplify the characteristic features of the electronic structure of these compounds with the DOS of V_8Ga_{41}[7] shown in Figure 1 a: At low energy the density of states is dominated by approximately parabolically distributed (free-electron like) states stemming from the sp bands of the E atom matrix, which at higher energy are perturbed by the T atom d states. The strong d – sp interaction in these compounds opens up a pseudo gap (or sometimes even a narrow band gap) at or close to the Fermi level (E_F) which separates d – sp bonding and antibonding states. Figure 1 b summarizes in a simplified manner how the DOS of the T_mE_n Hume – Rothery compounds is built up by this perturbation process. As a consequence the TE_p coordination polyhedra represent strongly bonded entities, and the position of the pseudo gap determines the optimum VEC, or in the case of broad pseudo gaps a range of optimum VECs, for a particular Hume – Rothery compound. In V_8Ga_{41}[8] only one kind of TE_p polyhedron—corresponding to a VGa_{10} unit—occurs. This

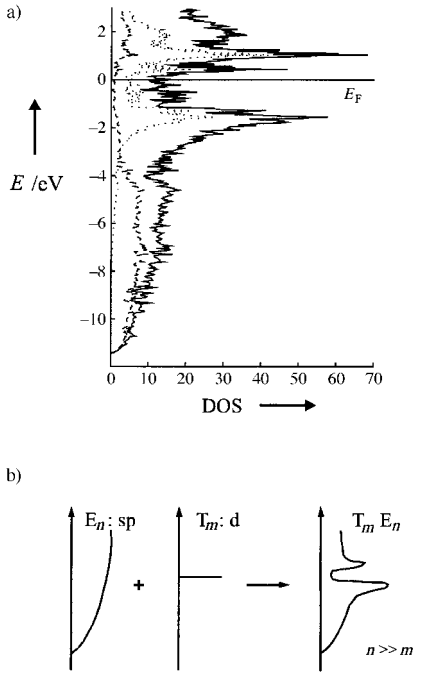

Figure 1. a) Total density of states (DOS (states/eV cell)) together with the d orbital contribution from V (dotted lines) and the s orbital contribution from Ga (dashed lines) of the compound V_8Ga_{41} as obtained from LMTO – ASA calculations. b) Schematical construction of the DOS of the T_mE_n Hume – Rothery compounds as a perturbation of free-electron like states of the E atom matrix by T atom d states.

[*] Dr. U. Häussermann, Prof. S. Lidin
Department of Inorganic Chemistry, Stockholm University
10691 Stockholm (Sweden)
Fax: (+46) 8-152187
E-mail: ulrich@inorg.su.se
Dr. P. Viklund, Dr. C. Svensson
Department of Inorganic Chemistry 2
Lund University (Sweden)
S. Eriksson
Studsvik Neutron Research Laboratory
Uppsala University (Sweden)
Dr. P. Berastegui
ISIS Facility, Rutherford Appleton Laboratory
Chilton, Didcot, Oxon (UK)

[**] This work was supported by the Swedish National Science Research Council (NFR) and the Göran Gustafsson Foundation.

  1433-7851/99/3804-0488 $ 17.50+.50/0

VGa_{10} coordination polyhedron represents a hybrid composed of one half of a cube ($VGa_{8/2}$) and one half of an icosahedron ($VGa_{12/2}$)[9] and is depicted in Figure 2a. In the V_8Ga_{41} structure these polyhedra exclusively share corners (Figure 2b) and are arranged in such a way that one triangular

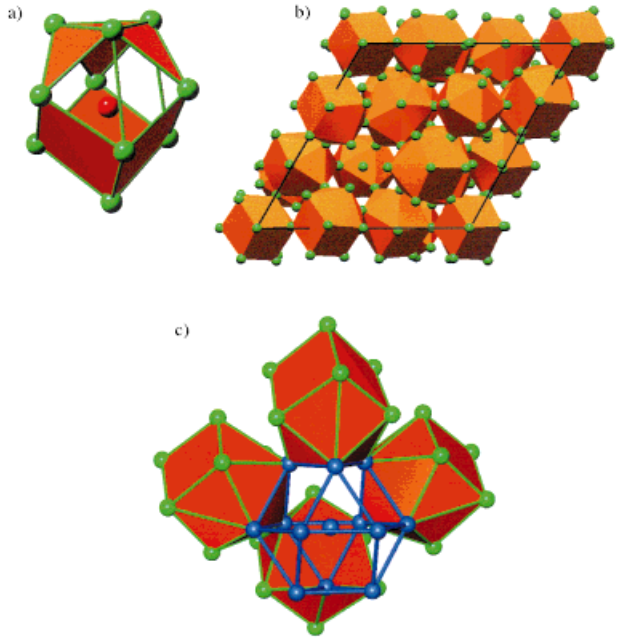

Figure 2. a) The hybrid coordination polyhedron of the V atoms in V_8Ga_{41} consisting of one half of a cube (lower part) and one half on an icosahedron (upper part). b) The structure of V_8Ga_{41} along [001] build up by corner-sharing VGa_{10} polyhedra (red). c) The cuboctahedron in V_8Ga_{41} defined by eight VGa_{10} hybrid polyhedra (only four of them are shown for clarity).[17]

face of each polyhedron is at the same time part of a cuboctahedron which is centered by an additional Ga atom. Thus such a cuboctahedron is defined by eight VGa_{10} polyhedra (Figure 2c) which yields the stoichiometry $Ga(VGa_{10/2})_8 = V_8Ga_{41}$ for this compound.

In the course of our investigation of the stability ranges of Hume–Rothery compounds we obtained the new phase $Mn_8Ga_{41-x}Zn_x$ from Zn/Ga melts[10] with a rather narrow homogeneity range[11] which can be regarded as a $T_mE_{n-x}E'_x$ Hume–Rothery compound. The X-ray structure determination[12] of a single crystal from a sample with the nominal composition $Mn_4Zn_{32}Ga_{64}$ exhibited a rhombohedral structure for a compound $Mn_8Ga_{\approx 27}Zn_{\approx 14}$ which at first sight appeared as a simple ternary variant of the V_8Ga_{41} structure where Ga atoms in the E atom matrix have partly been replaced by Zn atoms. When counting Zn as an E atom that only contributes to bonding with its 4s electrons one might consider a random replacement of Ga with the neighboring element Zn as a means to balance the increase of VEC due to the electron richer T component in $Mn_8Ga_{41-x}Zn_x$. Then VEC yields a value of 3.367 in $Mn_8Ga_{27}Zn_{14}$, which is slightly higher than that in V_8Ga_{41} but the Fermi level would still be within the pseudo gap of V_8Ga_{41} when assuming a rigid-band behavior of the band structure (Figure 1). In order to be able to discriminate reliably between Ga and Zn atoms and to investigate their distribution in the E atom matrix we performed a neutron powder diffraction study.[13] The Rietveld refinement (Figure 3) revealed an average composition $Mn_8Ga_{27.4(1)}Zn_{13.6(1)}$ of the crystals from the sample $Mn_4Zn_{32}Ga_{64}$ and an intriguing segregation of the Zn and Ga atoms in the E atom substructure of $Mn_8Ga_{27.4}Zn_{13.6}$.[14] This, together with some small but decisive geometric

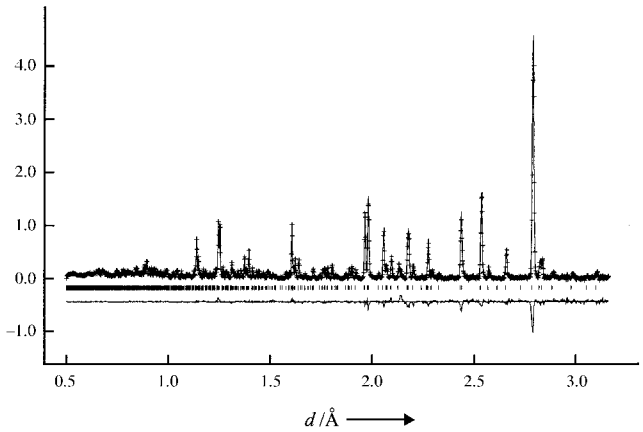

Figure 3. The Rietveld-fitted profile and difference plot (time-of-flight neutron powder diffraction data) for $Mn_8Ga_{27.4}Zn_{13.6}$. The vertical axis shows counts per μs.

deviations from the parent V_8Ga_{41} type turns the ternary $Mn_8Ga_{27.4}Zn_{13.6}$ into a very remarkable structure. The most remarkable feature of $Mn_8Ga_{27.4}Zn_{13.6}$ is the occurrence of separated $Zn_{12}E$ cluster entities; that is, the two atomic positions defining the cuboctahedron are exclusively occupied by Zn atoms (positions Zn1 and Zn2), and the center of these clusters represents the only significantly detected random occupied atomic position in this structure (position E: 61(9)% Zn and 39(9)% Ga). Moreover, the distances between neighboring atoms in the $Zn_{12}E$ clusters are in the very narrow range between 2.754 and 2.814 Å (d(E–Zn1) 2.790 (6×), d(E–Zn2) 2.779 (6×), d(Zn1–Zn1) 2.790 (6×), d(Zn1–Zn2) 2.780 (6×), 2.814 (6×), d(Zn2–Zn2) 2.754 Å (6×)) compared to the range of 2.885 to 3.034 Å between the corresponding pairs of Ga atoms in V_8Ga_{41}.[8] As a consequence of this idealization of the cuboctahedral units in $Mn_8Ga_{27.4}Zn_{13.6}$ the distances between Mn and the Zn atoms of the cuboctahedra are enlarged and the MnE_{10} polyhedra appear as more distorted than their VGa_{10} counterparts in V_8Ga_{41}. Thus the $Zn_{12}E$ clusters in $Mn_8Ga_{27.4}Zn_{13.6}$ can be regarded as small volumes of face-centered cubic metal which are separated by at least 3.929 Å as the shortest distance between Zn atoms belonging to neighboring cuboctahedra; the distance between the centers of the clusters is 9.240 Å. The mean distance between neighboring atoms in the centered cuboctahedra is 2.785 Å, which compares very well with the mean interatomic distance of 2.789 Å between nearest neighbors in the elemental structure of Zn. Thus, $Mn_8Ga_{27.4}Zn_{13.6}$ appears not only as an ordinary variant of the binary Hume–Rothery compound V_8Ga_{41} where the exchange of Ga by Zn supplies an optimum value of VEC, but exhibits a subtle ordering tendency of Ga and Zn in the flexible E atom substructure which accounts for the different

  1433-7851/99/3804-0489 $ 17.50+.50/0

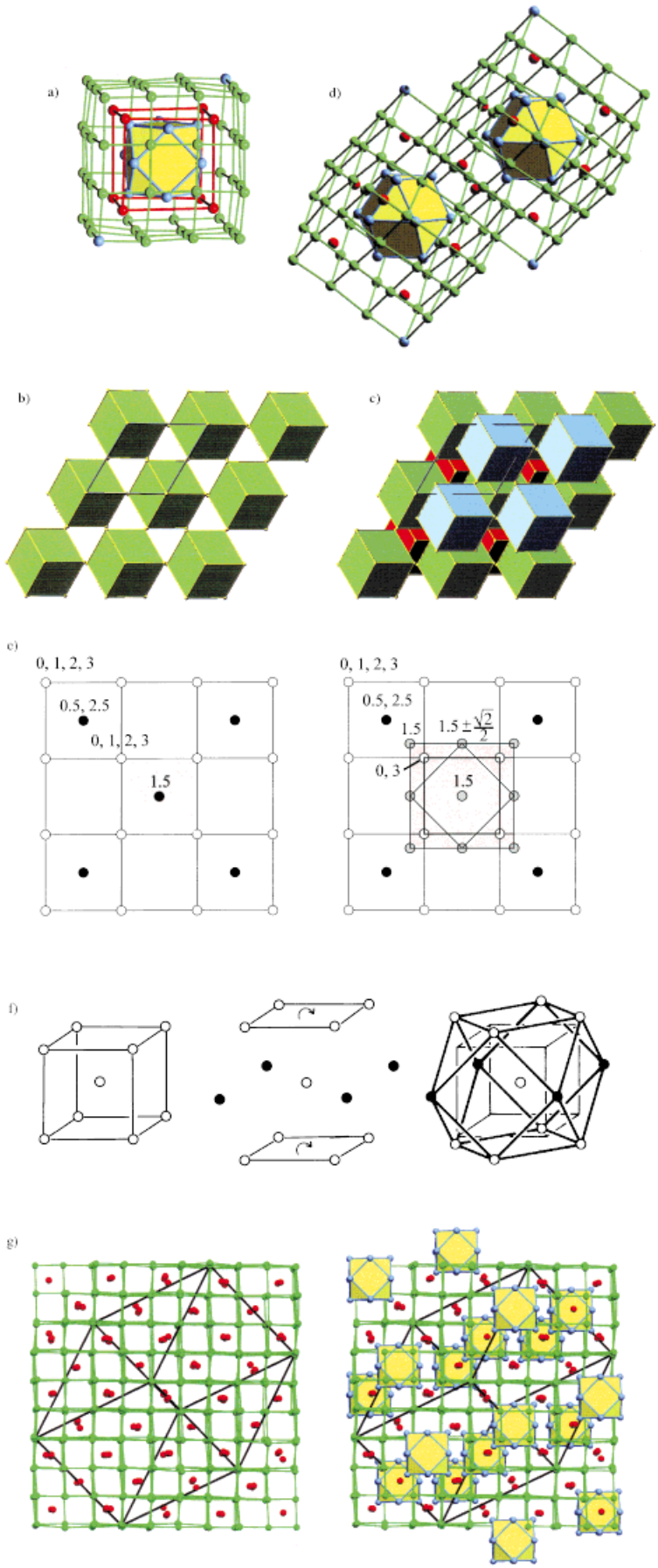

bonding behavior of these elements: the tendency of Ga to form homonuclear E–E and heteronuclear T–E bonds and the tendency of Zn to segregate into more metallic bonded entities. In contrast to the V_8Ga_{41} structure in which strong-bonded VGa_{10} polyhedra are the essential building units, for $Mn_8Ga_{27.4}Zn_{13.6}$ we assign this role to the centered cuboctahedra $Zn_{12}E$. When focussing on these cluster entities as the central structural units it is possible to define a large three-shell building block consisting of 77 atoms. The interior of such a building block (Figure 4a) is formed by a $Zn_{12}E$ cluster, and eight Mn atoms which coordinate the triangular faces of the cuboctahedron constitute its second shell. Thus the Mn atoms are arranged as a cube, which is slightly distorted, and the average distance between two Mn atoms is 5.21 Å. The outer shell or surface of the large building block consists of 56 E atoms (54 Ga atoms and two Zn atoms (position Zn3)) and has also the shape of a (slightly distorted) cube, exhibiting the same orientation as the inner cube formed by the Mn atoms.

This large "supercube" is equivalent in volume and shape to the primitive rhombohedral unit cell of $Mn_8Ga_{27.4}Zn_{13.6}$ with $a = 9.240$ Å and $\alpha = 95.80°$, but with a different orientation (cf. Figure 4b). On each face of a supercube 16 E atoms are located which divide the area into 3×3 smaller arrays. The two Zn3 atoms sit on opposite corners ((0,0,0) and (1,1,1)) along a body diagonal (cf. Figure 4a) and the distance between these atoms and the closest Zn atoms of the $Zn_{12}E$ cluster in the center of the building block is 5.269 Å. The total composition of the stuffed supercube is T_8E_{69} and such building blocks composed of three shells might even occur in the formation process of the compound in the Zn/Ga (E atom) melt, starting off the centered cuboctahedra $Zn_{12}E$ as nucleation centers. In the hexagonal setting of the $Mn_8Ga_{27.4}Zn_{13.6}$ structure the stuffed supercubes are oriented along the body diagonal defined by the two Zn3 atoms. This orientation corresponds to the *c* axis, and the

Figure 4. a) The stuffed "supercube" building block in $Mn_8Ga_{27.4}Zn_{13.6}$. The inner shell represents a centered $Zn_{12}E$ cuboctahedron (yellow), the second shell corresponds to a cube of eight Mn atoms (red circles), and the outer shell to a cube with 56 E atoms (54 Ga (green circles) and two Zn atoms (blue circles)) on its surface. b) Layer of hexagonally arranged stuffed supercubes, oriented along a body diagonal (*c* direction) and not connected, in $Mn_8Ga_{27.4}Zn_{13.6}$. c) ABC stacking of layers of stuffed supercubes yield the total structure of $Mn_8Ga_{27.4}Zn_{13.6}$. d) Two condensed stuffed supercubes in two consecutive layers AB of $Mn_8Ga_{27.4}Zn_{13.6}$. e) From the $PtHg_4$ structure ($MnGa_4$) to the stuffed "supercube" building block in $Mn_8Ga_{27.4}Zn_{13.6}$. Black circles represent Mn atoms, lighter circles E atoms. The heights of the atoms are indicated. f) Generation of a cuboctahedron from a cube after Hyde and Andersson.[15] g) Left: part of the structure of $Mn_8Ga_{27.4}Zn_{13.6}$ which corresponds to the $PtHg_4$ type (red circles: Mn atoms (Pt), green circles: E atoms (Hg)); right: $Mn_8Ga_{27.4}Zn_{13.6}$-interspersed $Zn_{12}E$ clusters (yellow) in a primitive cubic host lattice.

  1433-7851/99/3804-0490 $ 17.50+.50/0

distance between the two Zn3 atoms is the repeating unit in this direction. The supercubes are arranged in hexagonally packed layers as indicated in Figure 4b, but are not connected within such a layer. The complete structure of $Mn_8Ga_{27.4}Zn_{13.6}$ results from an ABC stacking of such layers in the *c* direction (Figure 4c). Within the sequence ABC, supercubes are condensed in the *ab* plane by sharing 9 of the 16 E atoms located on each face, equivalent to 4/9 of the area of the face (Figure 4d). Thus each building unit is surrounded octahedrally by six neighbors in such a partly face-sharing way. The shared atoms are always Ga atoms, whereas the remaining (Zn3) atoms situated at opposite corners at the heights $z = 0$, ⅔, ⅔ are used to connect supercubes in the *c* direction.

The structural description of $Mn_8Ga_{27.4}Zn_{13.6}$ in terms of stuffed supercubes reveals the close connection of this structure with the $PtHg_4$ type in which also the compound $MnGa_4$ crystallizes. The cubic $PtHg_4$ type can be regarded as a defect CsCl structure where ¾ of the Cs atoms have been removed in such a way that an array of corner-connected cubes [$PtHg_8$] ([$MnGa_8$]) is formed (Figure 4e). The stuffed supercube in $Mn_8Ga_{27.4}Zn_{13.6}$ corresponds to a volume 1.5^3 times that of the body-centered unit cell of $MnGa_4$ of which the atoms defining the central cube [$MnGa_8$] has been replaced by the $Zn_{12}E$ cluster. The transformation process from a cube to a cuboctahedron is simple and was described by Hyde and Andersson[15] (Figure 4f): First a square of four more (Zn) atoms is added at the height of the center of the cube. Then the cube is elongated in the direction perpendicular to the plane defined by the additional atoms and its remaining two square faces are rotated by 45° to yield a cuboctahedron. The generation of a cuboctahedron from a cube raises the coordination number of the surrounding Mn atoms from 8 to 10, which results in the hybrid coordination polyhedron shown in Figure 1a. Beyond this the $PtHg_4$ type host structure of $MnGa_4$ is unaffected and the $Zn_{12}E$ cluster in $Mn_8Ga_{27.4}Zn_{13.6}$ appear as separated, interspersed entities in a primitive cubic array in which the Ga atoms are segregated (Figure 4g).

The cubic primitive lattice is a perfect host for cuboctahedral units where square antiprims of flexible size serve as an interface and thus also allow some flexibility in the size of the cuboctahedra (cf. Figure 4e). For $Mn_8Ga_{27.4}Zn_{13.6}$, the distribution of the centered cuboctahedra formed by Zn atoms in the $MnGa_4$ host structure ensures for all Mn atoms the same coordination, but one could also think of a structural series T_nE_{4n} ($PtHg_4$ type host) $\rightarrow T_{n-1}E1_{4n-8}E2_{13}$ where T atoms occupy E_{10} hybrid polyhedra as well as cubes and E1 atoms participate in the cubic primitive lattice into which centered cuboctahedra (small volumes of face-centered cubic metal) formed by the E2 atoms are distributed. $Mn_8Ga_{27.4}Zn_{13.6}$ ($Mn_8[Ga_{27}Zn]Zn_{12}E$) would be the first member with $n = 9$. Such a homologous series with the same structural principle based on the fluorite type as host structure is, for example, known for the ionically bonded system CaF_2/YF_3, including the mineral tveitite $Ca_{14}Y_5F_{43}$, where "excess" fluoride ions form the centered cuboctahedra.[16]

Received: July 31, 1998 [Z 12233 IE]
German version: *Angew. Chem.* **1999**, *111*, 580 – 584

Keywords: bond theory · clusters · intermetallic phases · structure elucidation · zinc

[1] R. Nesper, *Angew. Chem.* **1991**, *103*, 805; *Angew. Chem. Int. Ed. Engl.* **1991**, *30*, 789, and references therein.
[2] G. J. Miller in *Chemistry, Structure and Bonding of Zintl Phases and Ions* (Ed.: S. M. Kauzlarich), VCH, New York, **1996**, pp. 1 – 59, and references therein.
[3] R. Ferro, A. Saccone in *Materials Science and Technology, Vol. 1 (The Structure of Solids)* (Eds.: R. W. Cahn, P. Haasen, E. J. Kramer), VCH, Weinheim, **1993**, pp. 123 – 215.
[4] The expression Hume – Rothery compound or Hume – Rothery phase for electron compound is frequently used by the physical community. It is not only restricted to the representatives of the specific structural series face-centered cubic → body-centered cubic → γ-brass → hexagonally close-packed, which is the classic example of VEC-controlled stability ranges in intermetallic systems.
[5] H. Hillebrecht, *Z. Kristallogr. Suppl.* **1994**, *8*, 340; M. Ade, H. Hillebrecht, *Z. Kristallogr. Suppl.* **1995**, *10*, 101; H. Hillebrecht, V. Kuntze, K. Gebhardt, *Z. Kristallogr.* **1997**, *212*, 840.
[6] G. Trambly de Laissardière, D. Nguyen Manh, L. Magaud, J. P. Julien, F. Cyrot-Lackmann, D. Mayou, *Phys. Rev. B* **1995**, *52*, 7920.
[7] The density of states of V_8Ga_{41} was calculated self-consistently using the local density-functional approximation and the scalar relativistic linear muffin-tin orbital (LMTO) method in the atomic sphere approximation (ASA) (M. van Schilfgarde, T. A. Paxton, O. Jepsen, G. Krier, A. Burkhard, O. K. Andersen, *Program TB-LMTO 4.6*; Max-Planck Institut Stuttgart, Stuttgart, **1994**). The exchange-correlation potential was parametrized according to von Barth and Hedin (U. von Barth, L. Hedin, *J. Phys. C* **1972**, *5*, 1629). The reciprocal space integrations were performed with the tetrahedron method (O. Jepsen, O. K. Andersen, *Solid State Commun.* **1971**, *9*, 1763) using 40 irreducible *k*-points.
[8] K. Girgis, W. Peter, G. Pupp, *Acta Crystallogr. Sect. B* **1975**, *31*, 113.
[9] K. Yvon, *Acta Crystallogr. Sect. B* **1975**, *31*, 117.
[10] The phase $Mn_8Ga_{41-x}Zn_x$ ($\approx 14 < x < \approx 16$) was prepared from mixtures of the pure elements containing 1 mmol Mn and a total amount of 20 mmol E component with various ratios Zn/Ga. The reactants were pressed into pellets and loaded into quartz ampoules, which were sealed under vacuum. The samples were heated to 600 °C for 60 h and then slowly cooled to room temperature at an approximate rate of 10 °C h^{-1}. Excess E metal was dissolved with 4 M HCl. The homogeneity of the crystalline product was confirmed by powder X-ray diffraction. Mixtures with a Ga/Zn ratio larger than 3 yielded the compound $MnGa_4$ and virtually no $Mn_8Ga_{41-x}Zn_x$.
[11] The homogeneity range of $Mn_8Ga_{41-x}Zn_x$ was estimated to be $\approx 14 < x < \approx 16$ by means of semiquantitative elemental analyses of crystals from samples with different Zn/Ga ratios with the energy disperse X-Ray (EDX) method in a JEOL scanning microscope.
[12] Crystal structure determination of $Mn_8Ga_{\approx 27}Zn_{\approx 14}$ from a sample $Mn_4Zn_{32}Ga_{64}$, silvery cube-shaped or tabular crystals, crystal size: $0.1 \times 0.06 \times 0.06$ mm^3, $a = 13.6033(6)$, $c = 14.6058(16)$ Å (based on least squares from 30 measured and indexed lines of a Guinier powder diagram ($Cu_{K\alpha}$, Si (NIST) standard)), $\rho_{calcd} = 6.889$ g cm^{-3}, rhombohedral, space group $R\bar{3}$ (No. 148), $Z = 3$, Siemens SMART CCD diffractometer (Siemens Analytical X-ray Instruments Inc. *SMART Reference Manual*, Madison, Wisconsin, USA, **1996**), $Mo_{K\alpha}$ radiation, $\mu = 36.45$ mm^{-1}, data reduction with SAINT (Siemens Analytical X-ray Instruments Inc. ASTRO and SAINT: Data Collection and Processing Software for the SMART System, Madison, Wisconsin, USA, **1995**), absorption correction with SADABS (G. M. Sheldrick, *SADABS User Guide*, Universität Göttingen, **1996**), 31809 measured reflections ($2° < 2\theta < 110.63°$), 6678 unique reflections ($R_{int} = 0.062$), structure determination with direct methods (G. M. Sheldrick, SHELXL-86 Program for the Solution of Crystal Structures, Universität Göttingen, **1990**), structure refinement against F^2 (G. M. Sheldrick, SHELXL-93 Program for the Refinement of Crystal Structures, Universität Göttingen, **1993**), 79 parameters, $w = [\sigma^2(|F_o|^2) + (0.0423\,P)^2 + 3.03\,P]^{-1}$, R for 4737 $F_o > 4\sigma(F_o) = 0.0383$, $R_w(F^2)$ for all

6678 data = 0.094, GOF = 1.019, largest hole and peak = −2.72 and 2.38 e Å^{-3}. The refinement of the occupancies for the Ga and Zn positions gave the tentative composition $Mn_8Ga_{\approx 27}Zn_{\approx 14}$ which coincides with the Ga/Zn ratio of the reaction mixture. Further details of the crystal structure investigation can be obtained from the Fachinformationszentrum Karlsruhe, D-76344 Eggenstein-Leopoldshafen, Germany (fax: (+49) 7247-808-666; e-mail: crysdata@fiz-karlsruhe.de), on quoting the depository number CSD-410318.

[13] The neutron scattering lengths of Ga and Zn differ by about 20%. Time-of-flight neutron powder diffraction data was collected at room temperature using the POLARIS diffractometer at the ISIS Facility, UK. The backscattering detector bank which covers the scattering angles $130^\circ < 2\theta < 160^\circ$ was used, providing data over the *d*-spacing range $0.2 < d < 3.2$ Å with a resolution of $\Delta d\, d^{-1} = 5 \times 10^{-3}$. The normalized diffraction data was corrected for absorption.

[14] Rietveld analysis was carried out using the program GSAS (A. C. Larson, R. B. von Dreele, M. Lujan, *GSAS: The General Structure Analysis System*, Los Alamos National Laboratory, Los Alamos, NM, **1994**). The refined parameters included an extinction correction. Due to a strong correlation between temperature factors and occupancies, only two temperature factors, for the Mn and Ga atoms and for Zn atoms, respectively, were refined (3687 data points, $R_p = 0.0452$, $R_{wp} = 0.0216$, $\chi^2 = 1.982$ (for 38 variables), $R_p = \Sigma |y_{oi} - y_{ci}| / \Sigma |y_{oi}|$, $R_{wp} = (\Sigma w |y_{oi} - y_{ci}|^2 / \Sigma w |y_{oi}|^2)^{0.5}$.

[15] B. G. Hyde, S. Andersson, *Inorganic Crystal Structures*, Wiley, New York, **1989**, p. 196.

[16] D. J. Bevan, O. Greis, J. Strähle, *Acta Crystallogr. Sect. A* **1980**, *36*, 889.

[17] P. Hofmann, R. Nesper, COLTURE: program for interactive visualisation of crystal structures, ETH Zürich, Zürich, **1995**.

Helical Coordination Polymers with Large Chiral Cavities**

Kumar Biradha, Corey Seward, and Michael J. Zaworotko*

The concept of crystal engineering[1, 2] owes much to recent advancements in supramolecular chemistry and recognition, understanding, and exploitation of supramolecular synthons.[3] Crystal engineering offers the intriguing promise of facile development of a new generation of functional solids that have been designed from first principles. Therefore, a degree of control over substrates, structure and, ultimately, bulk properties that is not inherently present in naturally occurring compounds is potentially offered. Furthermore, it is already clear that the construction of architectures that are unprecedented in naturally occurring solids becomes feasible. In the context of metal-organic solids, infinite molecular brick walls,[4] ladders,[5] bilayers,[6] and helices[7, 8] represent just four examples of this new generation of solids. Of particular current interest are these and other examples of open framework metal-organic[9, 10] and organic[11, 12] zeolite mimics which incorporate organic guests and "organic clay mimics" which are able to exchange metal cations.[13] Herein we report on a new class of host compound, helical coordination polymers that spontaneously resolve to generate chiral cavities that are large enough to contain supramolecular complexes of organic guest molecules. Significantly, these chiral architectures are generated from simple and inexpensive achiral building blocks.

A weak but commonly encountered supramolecular synthon is the T-shape or edge-to-face stacking interaction.[14] This type of C−H $\cdots$ π interaction[15] occurs, for example, in the crystal structure of benzene and appears to be the key driving force for the architecture that is exhibited by the simple and facile to synthesize compound **1**. Crystals of **1** were grown by dissolving [Ni(acetate)$_2$] and benzoic acid in MeOH and layering with a solution of 4,4′-dipy in MeOH [Eq. (1); 4,4′-dipy = 4,4′-bipyridine].

$$Ni(CH_3COO)_2 \cdot 4H_2O + 4,4'\text{-dipy} \xrightarrow{ArCOOH,\ MeOH} [\{Ni(4,4'\text{-dipy})(ArCOO)_2(MeOH)_2\}_n] \quad (1)$$

1: Ar = C_6H_5
2: Ar = 2-(OH)C_6H_4
3: Ar = 3-(NO_2)C_6H_4

An X-ray structure analysis[16] reveals that **1** acts as a host compound if crystals are grown in the presence of the guest molecules nitrobenzene, benzene, veratrole, phenol, chloroform, and dioxane to generate the inclusion compounds **1a–f**, respectively. These exhibit isostructural helical architectures with large chiral cavities. The helices are generated around crystallographic 4_1 or 4_3 screw axes and each coil of the helix therefore contains four residues (Figure 1). The distance between coils corresponds to the unit cell length, which ranges from 27.02 to 27.91 Å. As revealed by Scheme 1, this architecture is one of at least three possible architectures that might reasonably exist for **1**. Square boxes based upon 4,4′-dipy have attracted considerable recent attention,[17] but we are un-

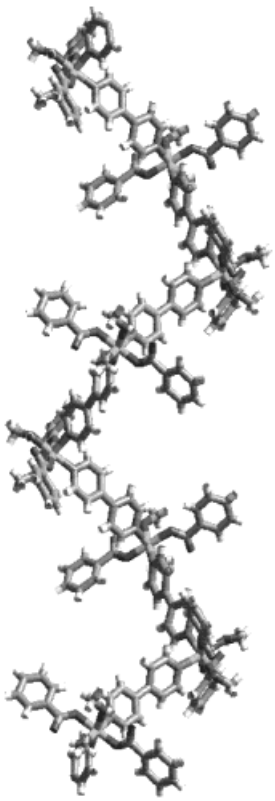

Figure 1. A portion of the helical structure exhibited by compounds **1a–f**.

[*] Prof. Dr. M. J. Zaworotko, Dr. K. Biradha, C. Seward
Department of Chemistry, The University of Winnipeg
515 Portage Avenue, Winnipeg, Manitoba, R3B 2E9 (Canada)
Fax: (+1) 204-783-7981
E-mail: mike.zaworotko@uwinnipeg.ca

[**] We thank the Environmental Science and Technology Alliance Canada (ESTAC) and the Natural Sciences and Engineering Research Council of Canada (NSERC) for providing financial support for this work.

  1433-7851/99/3804-0492 $ 17.50+.50/0